Out of the blue: volcanic SO2 emissions during the 2021-2022 Hunga Tonga - Hunga Ha'apai eruptions

Simon Carn[1], Nickolay Krotkov[2], Bradford Fisher[3], and Can Li[4]

[1]Michigan Technological University
[2]NASA Goddard Space Flight Center
[3]Science Systems and Applications
[4]University of Maryland

November 23, 2022

Abstract

The January 15, 2022 phreatomagmatic eruption of the submarine Hunga Tonga-Hunga Ha'apai (HTHH) volcano (Tonga) generated an explosion of historic magnitude, and was preceded by ˜1 month of Surtseyan eruptive activity and two precursory explosive eruptions. We present an analysis of ultraviolet (UV) satellite measurements of volcanic sulfur dioxide (SO2) between December 2021 and the climactic January 15, 2022 eruption, comprising an unprecedented record of Surtseyan eruptive emissions. UV measurements from the Ozone Monitoring Instrument (OMI) on NASA's Aura satellite, the Ozone Mapping and Profiler Suite (OMPS) on Suomi-NPP, the Tropospheric Monitoring Instrument (TROPOMI) on ESA's Sentinel-5P, and the Earth Polychromatic Imaging Camera (EPIC) aboard the Deep Space Climate Observatory (DSCOVR) are combined to yield a consistent multi-sensor record of SO2 emissions during the eruptive sequence. We estimate SO2 emissions during the key phases of the eruption: the initial December 19, 2021 eruption (˜0.01 Tg SO2); continuous SO2 emissions from December 20, 2021-early January 2022 (˜0.12 Tg SO2); the January 13, 2022 stratospheric eruption (0.06 Tg SO2); and the paroxysmal January 15, 2022 eruption (˜0.4-0.5 Tg SO2); yielding a total SO2 emission of ˜0.6-0.7 Tg SO2 for the entire eruptive episode. We interpret the vigorous SO2 emissions observed prior to the January 2022 eruptions, which were significantly higher than measured in the 2009 and 2014 HTHH eruptions, as strong evidence for a rejuvenated magmatic system. High cadence DSCOVR/EPIC SO2 imagery permits the first UV-based analysis of umbrella cloud spreading and volume flux in the January 13, 2022 eruption, and also tracks early dispersion of the stratospheric SO2 cloud injected by the January 15 eruption. The ˜0.4-0.5 Tg SO2 discharged by the paroxysmal January 15, 2022 HTHH eruption is low relative to other eruptions of similar magnitude, and a review of previous submarine eruptions of the satellite era indicates that such modest SO2 yield may be characteristic of these events, with the emissions and atmospheric impacts likely dominated by water vapor (WV). The origin of the low SO2 loading awaits further investigation but scrubbing of SO2 in the water-rich eruption plumes and rapid conversion to sulfate aerosol are highly plausible, given the exceptional WV emission measured in the January 15, 2022 HTHH eruption.

Out of the blue: volcanic SO_2 emissions during the 2021-2022 Hunga Tonga – Hunga Ha'apai eruptions

Carn, S.A.[1,*], N.A. Krotkov[2], B.L. Fisher[3], and C. Li[2,4]

[1]Department of Geological and Mining Engineering and Sciences, Michigan Technological University, Houghton, MI 49931, USA; scarn@mtu.edu
[2]Atmospheric Chemistry and Dynamics Laboratory, Code 614, NASA Goddard Space Flight Center, Greenbelt, MD 20771, USA
[3]Science Systems and Applications, Inc. (SSAI), Lanham, MD, USA
[4]Earth System Science Interdisciplinary Center, University of Maryland, College Park, MD, USA

*Corresponding author (scarn@mtu.edu)

Abstract

The January 15, 2022 phreatomagmatic eruption of the submarine Hunga Tonga-Hunga Ha'apai (HTHH) volcano (Tonga) generated an explosion of historic magnitude, and was preceded by ~1 month of Surtseyan eruptive activity and two precursory explosive eruptions. We present an analysis of ultraviolet (UV) satellite measurements of volcanic sulfur dioxide (SO_2) between December 2021 and the climactic January 15, 2022 eruption, comprising an unprecedented record of Surtseyan eruptive emissions. UV measurements from the Ozone Monitoring Instrument (OMI) on NASA's Aura satellite, the Ozone Mapping and Profiler Suite (OMPS) on Suomi-NPP, the Tropospheric Monitoring Instrument (TROPOMI) on ESA's Sentinel-5P, and the Earth Polychromatic Imaging Camera (EPIC) aboard the Deep Space Climate Observatory (DSCOVR) are combined to yield a consistent multi-sensor record of SO_2 emissions during the eruptive sequence. We estimate SO_2 emissions during the key phases of the eruption: the initial December 19, 2021 eruption (~0.01 Tg SO_2); continuous SO_2 emissions from December 20, 2021 – early January 2022 (~0.12 Tg SO_2); the January 13, 2022 stratospheric eruption (0.06 Tg SO_2); and the paroxysmal January 15, 2022 eruption (~0.4-0.5 Tg SO_2); yielding a total SO_2 emission of ~0.6-0.7 Tg SO_2 for the entire eruptive episode. We interpret the vigorous SO_2 emissions observed prior to the January 2022 eruptions, which were significantly higher than measured in the 2009 and 2014 HTHH eruptions, as strong evidence for a rejuvenated magmatic system. High cadence DSCOVR/EPIC SO_2 imagery permits the first UV-based analysis of umbrella cloud spreading and volume flux in the January 13, 2022 eruption, and also tracks early dispersion of the stratospheric SO_2 cloud injected by the January 15 eruption. The ~0.4-0.5 Tg SO_2 discharged by the paroxysmal January 15, 2022 HTHH eruption is low relative to other eruptions of similar magnitude, and a review of previous submarine eruptions of the satellite era indicates that such modest SO_2 yield

may be characteristic of these events, with the emissions and atmospheric impacts likely dominated by water vapor (WV). The origin of the low SO_2 loading awaits further investigation but scrubbing of SO_2 in the water-rich eruption plumes and rapid conversion to sulfate aerosol are highly plausible, given the exceptional WV emission measured in the January 15, 2022 HTHH eruption.

1. Introduction

The vast majority of active volcanism on Earth is submarine; a realm where the eruption products are inaccessible to remote sensing techniques that use electromagnetic radiation. Submarine volcanic emissions thus remain largely undetected or unquantified, except in the relatively rare cases when submarine eruptions generate pumice rafts or volcanic plumes that breach the ocean surface and rise into the atmosphere [e.g., *Cahalan and Dufek*, 2021]. The latter occurred in dramatic fashion during the January 15, 2022 eruption of Hunga Tonga – Hunga Ha'apai (HTHH), a submarine volcano in Tonga. The January 15, 2022 HTHH eruption, which was the culmination of an eruptive sequence that began in December 2021, produced an eruption column with overshooting tops that rose to lower mesospheric altitudes (~55 km) [*Carr et al*., 2022], an umbrella cloud that rivalled the 1991 Pinatubo eruption in horizontal extent, a plethora of atmospheric waves that propagated globally [*Matoza et al*., 2022; *Wright et al*., 2022], vigorous lightning, and local and distal tsunamis [*Kubota et al*., 2022]. The highly explosive nature of the 2022 HTHH eruption was driven by violent magma-seawater interaction, and the event drew comparisons with the 1883 eruption of Krakatau (Indonesia), which produced some analogous atmospheric phenomena [*Symons*, 1888]. Analysis of the 2022 HTHH eruption therefore provides an unprecedented opportunity to gain insight into violent, shallow submarine eruptions such as the

1883 Krakatau event, and into the potential hazards and atmospheric impacts of explosive submarine volcanism.

Here, we present an analysis of sulfur dioxide (SO_2) measurements collected by ultraviolet (UV) satellite instruments during the 2021-2022 eruptive sequence at HTHH, culminating in the paroxysmal January 15, 2022 event. The aim is to estimate total SO_2 emissions during the HTHH eruptions to aid assessments of their impacts on the atmosphere and climate, and to gain insight into trends in SO_2 emissions prior to the paroxysmal January 15, 2022 eruption. We also provide a new analysis of SO_2 emissions associated with other submarine volcanic eruptions in the UV satellite era (since 1978) to place the HTHH eruption in context.

3. 2021-2022 HTHH eruption

The islands of Hunga Tonga and Hunga Ha'apai (20.536ºS, 175.382ºW; elevation 114 m) are the subaerial fragments of the massive, submarine Hunga volcano that rises more than 2000 meters from the surrounding seafloor in the Tofua volcanic arc [*Cronin et al.*, 2017]. Prior to 2021-22, confirmed eruptions of HTHH occurred in June 1988, March 2009, and December 2014 [*Global Volcanism Program*, 2013], with the latter two eruptions including periods of island growth and erosion [*Vaughan and Webley*, 2010; *Garvin et al.*, 2018]. The typical eruption style of HTHH is the rarely observed Surtseyan style of activity, involving magma-seawater interaction, ephemeral island growth, and emission of volcanic plumes rich in water vapor and condensed water.

The 2021-2022 HTHH eruption sequence began abruptly on December 20, 2021 at 09:35 local time in Tonga (20:35 UTC on December 19) with what was (at the time) a significant explosive eruption for HTHH, though this event was much smaller than the subsequent explosive eruptions in January 2022. As we document below, the December 2021 eruption was followed by a period of near-continuous Surtseyan eruptive activity and SO_2 emissions that continued until early January 2022. After a 7-10 day lull in significant subaerial activity, another major explosive eruption occurred on January 13 at 15:20 UTC, followed by the paroxysmal event at 04:00 UTC on January 15.

4. Satellite data

The satellite SO_2 data used here are derived from four operational UV satellite sensors: the Ozone Monitoring Instrument (OMI), operating on NASA's Aura satellite since 2004 [*Levelt et al.*, 2018]; the Ozone Mapping and Profiler Suite (OMPS), operating on the NASA/NOAA Suomi-NPP satellite since 2012 [*Carn et al.*, 2015]; the Earth Polychromatic Imaging Camera (EPIC), observing Earth from the Deep Space Climate Observatory (DSCOVR) at the L1 Earth-Sun Lagrange point (1,000,000 miles from Earth) since 2015 [*Marshak et al.*, 2018]; and the Tropospheric Monitoring Instrument (TROPOMI), operating on ESA's Sentinel-5 Precursor (S5P) satellite since 2017 [*Veefkind et al.*, 2012]. Some key characteristics of these instruments are given in Table 1. OMI, OMPS and TROPOMI are aboard polar-orbiting satellites and hence have daily temporal resolution at the tropical latitudes of Tonga, whereas DSCOVR/EPIC collects high cadence UV imagery and, as we demonstrate here, provides novel insight into the HTHH eruptions. During the 2021-2022 HTHH eruptions, DSCOVR was in 'winter cadence' mode, providing UV images every ~110 minutes [*Herman et al.*, 2018].

Whilst all the UV instruments used here use backscattered UV radiation to retrieve vertical column densities (VCDs) of volcanic SO_2, differences in SO_2 sensitivity arise from variable spectral and spatial resolution and retrieval algorithms (Table 1). OMI, OMPS and TROPOMI are hyperspectral UV sensors capable of detecting VCDs of less than 1 Dobson Unit (DU; 1 DU =

2.69×10^{16} molecules cm^{-2}) in a single pixel [*Li et al.*, 2017; *Theys et al.*, 2017]; hence the relative sensitivity of these sensors to SO_2 mass is governed mainly by pixel size, with TROPOMI providing the highest spatial resolution (Table 1). DSCOVR/EPIC is a multi-spectral instrument with lower sensitivity to SO_2 (~5-10 DU per pixel; *Fisher et al.*, 2019) but with the advantage of higher temporal resolution (Table 1). All UV SO_2 retrievals require an assumption of SO_2 plume altitude; current operational Level 2 (L2) SO_2 products from OMI, OMPS and TROPOMI provide volcanic SO_2 VCDs assuming center of mass altitudes (CMAs) of ~8 km (mid-troposphere; TRM) and ~17 km (lower stratosphere; STL), which are most applicable to the explosive HTHH eruption. OMI and OMPS SO_2 data also include a lower tropospheric (TRL) SO_2 product (CMA = 3 km), which we have used to quantify SO_2 emissions from the HTHH activity in December 2021 – early January 2022. DSCOVR/EPIC SO_2 retrievals assume an upper tropospheric SO_2 CMA of 13 km [*Fisher et al.*, 2019]. Given the unusually high SO_2 injection altitude (outside the range of operational UV retrievals) and the presence of aerosols and ice in the HTHH volcanic clouds, we suggest an estimated uncertainty on the SO_2 measurements of ~35%.

All SO_2 products used here are publicly available via the NASA Earthdata portal (https://search.earthdata.nasa.gov/search). We use the Version 003 OMI L2 SO_2 product (OMSO2_003), the Version 2 OMPS Principal Component Analysis (PCA) SO_2 product (OMPS_NPP_NMSO2_PCA_L2_2) and the Version 2 DSCOVR/EPIC SO_2 product (DSCOVR_EPIC_L2_SO2_02). TROPOMI SO_2 data are derived from the Offline L2 SO_2 product (S5P_OFFL_L2__SO2), available from NASA Earthdata or the Sentinel-5P Pre-Operations Data Hub (https://s5phub.copernicus.eu/dhus/#/home). Measurements of SO_2 emissions for other volcanic eruptions of the satellite era are derived from Version 4 of the NASA MEaSUREs Multi-Satellite Volcanic SO_2 Level 4 Long-Term Global database (MSVOLSO2L4; *Carn*, 2022).

5. Results

Here, we summarize the UV satellite SO_2 measurements in chronological order of the 2021-2022 HTHH eruption sequence (local time in Tonga is 13 hours ahead of UTC). Daily SO_2 measurements from OMI, OMPS, TROPOMI or DSCOVR/EPIC are provided in Table 2.

5.1. The December 20, 2021 eruption

At the time, the eruption of HTHH at 20:35 UTC on December 19, 2021 (09:35 local time on December 20), was a significant event for the volcano, generating a steam-rich eruption plume that rose to the upper troposphere (~16 km altitude), accompanied by lightning, ash emissions and audible explosions [*Global Volcanism Program*, 2021a]. Due to its high temporal resolution, DSCOVR/EPIC detected SO_2 in the eruption plume as early as 20:53 UT on December 19 (~20 minutes after the eruption onset; Table 2), although SO_2 columns were close to the detection limit. Later OMI, OMPS and TROPOMI overpasses at 01:25-02:03 UTC measured ~0.01 Tg SO_2 in the volcanic plume (Table 2). The SO_2 emitted by this eruption continued to be detected by OMI, OMPS and TROPOMI for several days, confirming the relatively high altitude of injection where SO_2 lifetimes are longer [e.g., *Carn et al.*, 2016]. Based on the abrupt onset, high altitude plume, SO_2 loading, and subsequent activity (section 5.2) we posit that this eruption was driven by an injection of fresh magma into the volcano at shallow depths, promoting a phreatomagmatic eruption.

5.2. Continuous emissions: December 2021 – January 2022

Following the December 19 eruption, HTHH began a phase of continuous Surtseyan eruptive activity [*Global Volcanism Program*, 2021b, 2021c], accompanied by SO_2 emissions, that continued until January 2, 2022 (Table 2). In Table 2, we report daily SO_2 loadings measured in the HTHH eruption plumes by SNPP/OMPS, though similar SO_2 amounts were also measured by OMI and TROPOMI. Reported plume heights during this period of activity were variable, with peak heights reaching mid- to upper-tropospheric altitudes (Table 2), hence we have used the mid-tropospheric (TRM) OMPS SO_2 product to calculate SO_2 amounts.

The cumulative SO_2 mass measured by OMPS in this period (December 21, 2021 – January 2, 2022) is ~0.12 Tg SO_2, and given the water-rich, Surtseyan style of activity (with substantial scrubbing of SO_2 likely) we consider this a minimum estimate of actual SO_2 emissions. No SO_2 emissions were detected by OMI, OMPS or TROPOMI from January 3-6, 2022, though it is possible that heavy cloud cover over Tonga at this time obscured any plumes. Weak emissions of SO_2 resumed temporarily on January 7, and a few discrete 'puffs' of SO_2 were detected by TROPOMI on Jan 8-9 (Table 2). Although the latter contribute negligible amounts to the total SO_2 measured in this period, we interpret them as evidence of an at least partly 'open' volcanic system at this time, which may be significant in the context of the subsequent major explosive eruptions. After January 9, no further SO_2 emissions were detected until the major explosive eruption on January 13.

We note that the satellite SO_2 observations are broadly consistent with infrasound and hydrophone data reported by *Matoza et al.* [2022]. Infrasound generated by the HTHH activity was recorded continuously from December 19-31, 2021, coincident with the strongest SO_2 emissions (Table 2), and regular hydrophone detections of activity show a lull from January 4-13, 2022, which is also consistent with the observed decline in SO_2 discharge, suggesting that this is genuine. Overall, we find the SO_2 emissions measured in the December 21, 2021 – January 9, 2022 period, which were significantly higher than emissions measured at HTHH during prior eruptions in 2009 and 2014 (see Discussion; Table 4), to be strong evidence for a significant rejuvenation of the magmatic system at HTHH prior to the January 13-15 eruptions. This period of activity also involved substantial subaerial growth of the HTHH edifice

5.3. The January 13, 2022 eruption

The HTHH eruption at 15:20 UTC on January 13, 2022 (04:20 local time in Tonga on January 14) was larger than the December 19, 2021 event. It produced a lower stratospheric, water/ice-rich umbrella cloud that expanded to 240 km in diameter at 20 km altitude [*Global Volcanism Program*, 2022]. Based on umbrella cloud radius alone (~120 km), this eruption would rank as a Volcanic Explosivity Index (VEI) of 4, and it exceeds the cloud radii observed in many VEI 4 magmatic eruptions of recent years [*Constantinescu et al.*, 2021]. SO_2 emitted by the eruption was detected by all the UV satellite instruments, with a consistent peak total SO_2 mass of ~0.06 Tg measured by OMI, OMPS and TROPOMI (Table 2; Fig. 2, 3). Due to its lower SO_2 sensitivity, DSCOVR/EPIC measured a lower total SO_2 mass (~0.03 Tg), but we focus here on the unique high cadence UV EPIC observations of the umbrella cloud.

DSCOVR/EPIC first detected SO_2 in the January 13 eruption cloud at 19:56 UTC on January 13 (06:56 local time on January 14), ~4.3 hours after the eruption onset (Fig. 2a). This first EPIC SO_2 image (the first UV satellite measurement of the eruption by any sensor) shows a distinctive ‘ring-shaped’ cloud with SO_2 only detected at the margins of the expanding umbrella cloud, and SO_2 absent or below the EPIC detection limits (~5 DU) in the cloud core. Such an observation is highly unusual for a fresh eruption cloud, in which UV satellite measurements usually show high SO_2 columns, even in prior submarine eruptions such as at Bogoslof (Alaska, USA) in 2016-2017 [*Carn et al.*, 2017]. Hence, we interpret the EPIC SO_2 data as diagnostic of the water-rich, phreatomagmatic HTHH eruption in which SO_2 was significantly scrubbed or entirely stripped from the plume by co-emitted water (derived from the magma, seawater and/or entrained atmosphere). This conclusion is supported by the subsequent EPIC SO_2 measurements, which show radial spreading of the SO_2 signal, and confirms the presence of SO_2 in the umbrella cloud (Fig. 2b, c). At the time of the eruption, the closest available radiosonde soundings, from Pago Pago (American Samoa), show easterly winds in the lower stratosphere at 20 km altitude (Supplementary Figure S1); hence the EPIC SO_2 observation of SO_2 spreading east (i.e., upwind) is key. The EPIC measurements of umbrella cloud expansion with no concomitant increase in SO_2 mass loading (Table 2; Fig. 2) strongly suggests that most of the mass added to the umbrella during the eruption was highly water-rich. However, the early detection of SO_2 by EPIC also confirms some magmatic gas input, perhaps early in the eruption.

Using the EPIC SO_2 measurements (Table 3) it is possible to estimate the bulk volumetric flow rate of gas, ash and entrained atmosphere (V; m^3 s^{-1}) into the eruption plume using the *Woods and Kienle* [1994] gravity current model of an expanding umbrella cloud at the neutral buoyancy height:

$$R = \left[\frac{3\lambda NV}{2\pi}\right]^{1/3} t^{2/3}$$

where R is the radius of the plume (estimated here as an equivalent radius $R = \sqrt{(A/\pi)}$, where A is the non-circular SO_2 cloud area measured from the EPIC and TROPOMI SO_2 images in Fig. 2; Table 3), λ is an empirical constant related to the Froude number of the gravity current (where 0.2

is an appropriate value for tropical atmospheres [*Suzuki and Koyaguchi*, 2009]), *N* is the Brunt-Väisälä frequency or buoyancy frequency of the ambient atmosphere (s^{-1}), and *t* is the time since the onset of plume spreading (assumed to be 15:32 UTC on January 13, 2022). Using a Pago Pago radiosonde sounding at 12:00 UTC on January 13, we calculate a Brunt-Väisälä frequency of 0.026 s^{-1} at 20 km altitude for this case. Based on these values and a fit to the EPIC and TROPOMI data (Table 3), we obtain a volumetric flux of ~20 $km^3\ s^{-1}$. For comparison, *Prata et al.* [2020] report a volume flux of ~5 $km^3\ s^{-1}$ for the explosive phase of the 2018 Anak Krakatau eruption (Indonesia), which was also phreatomagmatic.

Prior analysis of umbrella cloud growth has been based on infrared (IR) geostationary (GEO) satellite imagery with higher temporal resolution than EPIC [e.g., *Van Eaton et al.*, 2016; *Prata et al.*, 2020]. Our study is the first attempt to use high-cadence UV imagery to analyze umbrella cloud growth, one key difference with prior work being that EPIC is sensitive to volcanic SO_2, whereas IR GEO measurements of volcanic cloud spread are based on the cloud-top brightness temperature of the bulk, opaque plume (i.e., a mixture of volcanic gas, ash, hydrometeors, etc.). We acknowledge that our analysis is limited by temporal resolution (i.e., the first EPIC SO_2 observation is >4 hours after the eruption onset, and hence missed any earlier umbrella growth phase, and EPIC's hourly cadence is lower than GEO sensors) and EPIC's sensitivity (i.e., the volcanic cloud could be larger in extent than shown in EPIC SO_2 data). However, although we might expect differences between volume fluxes calculated using the UV and IR satellite data, the availability of DSCOVR/EPIC SO_2 data offers the potential for wider application of this technique and may provide better sensitivity to volcanic clouds under certain conditions (e.g., gas-rich and ash-poor eruptions).

5.4. The January 15, 2022 eruption

Following the January 13 eruption, the bulk of the emitted SO_2 drifted west from Tonga under the influence of the easterly lower stratospheric winds (Fig. 3). The presence of the January 13 SO_2 cloud precludes detection of any SO_2 emissions between January 13 and 15 in UV satellite imagery, but inspection of geostationary GOES-West Advanced Baseline Imager (ABI) imagery (available in NASA Worldview; https://worldview.earthdata.nasa.gov/) reveals several strong 'puffs' from HTHH, on January 14 at 18:00 UTC and 21:10 UTC, and at 02:50 UTC on January 15, shortly before the major eruption. Hence sporadic emissions were clearly ongoing.

The paroxysmal HTHH eruption occurred at ~04:00 UTC on January 15, which is close to nightfall in Tonga (17:00 local time) and hence precluded early UV SO_2 observations of the nascent eruption cloud. A DSCOVR/EPIC exposure at 04:21 UTC, just ~20 minutes after the eruption, failed to detect any SO_2 due to the high solar zenith angle (SZA) or simply because the cloud was too small. Hence, in contrast to the January 13 eruption, analysis of umbrella cloud spread using the EPIC SO_2 data was not possible in this case. The first EPIC SO_2 observation on the following day (18:46 UTC on January 15; 09:46 local time on January 16 in Tonga) captured the eastern edge of the SO_2 cloud emitted by the January 15 eruption (Fig. 4). The next EPIC exposure at 20:34 UTC shows a ~200 km westward drift of the SO_2 cloud in the 108 minutes elapsed between the measurements (Fig. 4), indicating a wind speed of ~31 m/s. Such high wind speeds were only measured at altitudes above 30 km in the Pago Pago sounding (Supplementary Figure S2), consistent with other constraints on the injection altitude of the January 15 HTHH SO_2 cloud [e.g., *Millán et al.*, 2022].

Whilst the DSCOVR/EPIC data provide information on SO_2 cloud transport, the total SO_2 mass of ~0.2 Tg measured by EPIC at 20:34 UTC on January 15 is an underestimate of the actual

SO_2 loading due to the lower SO_2 VCDs than typically expected in a fresh volcanic cloud. More sensitive SNPP/OMPS observations at 01:53 UTC on January 16 measured ~0.4 Tg SO_2 in the volcanic cloud (Table 2; Fig. 3), though this also includes the ~0.06 Tg SO_2 emitted by the January 13 eruption, which is merged with the January 15 emissions. Very similar SO_2 amounts were measured by TROPOMI (Table 2).

SNPP/OMPS tracked the stratospheric volcanic SO_2 cloud produced by the January 13-15 HTHH eruptions for at least 10 days as it drifted west over Australia, the Indian Ocean and southern Africa (Fig. 3; Supplementary Movie). Figure 5 shows the trend in SO_2 mass retrieved using the OMPS data, which indicate an e-folding time of ~6 days. This is short relative to other tropical stratospheric eruptions observed in the satellite era [e.g., *Carn et al.*, 2016; *Zhu et al.*, 2020]. The January 15 HTHH eruption injected SO_2 to altitudes of over 30 km, where we would expect SO_2 lifetimes of ~30-40 days based on the 1982 El Chichón and 1991 Pinatubo eruptions. However, the submarine, phreatomagmatic HTHH eruption differs notably from these other, magmatic, eruptions in that it also injected a huge mass of water vapor into the mid-stratosphere, estimated at ~150 Tg H_2O by *Millán et al.* [2022] using Aura/Microwave Limb Sounder (MLS) data. As also proposed by other studies [e.g., *Zhu et al.*, 2022], we suspect that the relatively short lifetime of the HTHH SO_2 is due to this co-emitted water vapor, which acts as a source of OH that in turn catalyzes the oxidation of SO_2 to H_2SO_4 (sulfate) aerosol [*Glaze et al.*, 1997].

Using the observed SO_2 mass decay (Fig. 5) we can also estimate the initial erupted SO_2 mass by extrapolating the trend back to the time of the January 15 eruption, assuming a constant decay rate. This yields an initial SO_2 mass loading of ~0.49-0.54 Tg, and subtracting the 0.06 Tg SO_2 emitted on January 13 leaves 0.43-0.48 Tg SO_2 produced by the January 15 eruption. This is in very good agreement with the 0.41±0.02 Tg stratospheric SO_2 mass measured by Aura/MLS

[*Millán et al.*, 2022] and confirms that most or all the emitted SO_2 was injected into the stratosphere.

6. Discussion

6.1. Submarine volcanic eruptions of the satellite era

Here, we review available satellite measurements of SO_2 emissions for reported submarine eruptions in the satellite era (since 1978) to provide context for the 2021-2022 HTHH eruptions. As of April 2022, the Smithsonian Institution's Global Volcanism Program (GVP) reports 120 active Holocene submarine volcanoes, of which 80 have reported eruption dates and 40 last erupted since 1978 [*Global Volcanism Program*, 2013]. Volcano elevations for the 40 submarine volcanoes that have erupted since 1978 range from -4100 m (i.e., 4.1 km below sea level [bsl]) to 1.4 km above sea level with an average of ~0.9 km bsl. We note that elevations above sea level refer to the small, emergent portions of some submarine volcanic edifices, whereas the eruption vents are always below sea level. Some of the submarine volcanoes (e.g., HTHH, Home Reef and Lateiki [Tonga], Fukutoku-Oka-no-Ba [Japan]) have multiple reported eruptions since 1978, and it is perhaps not surprising that these are among the shallowest and hence more likely to produce plumes that breach the surface.

A review of global ultraviolet (UV) satellite SO_2 measurements since 1978 (*Carn*, 2022) reveals that ~12 submarine eruptions (not including the 2021-2022 HTHH eruptions) were sufficiently energetic to generate plumes that breached the ocean surface and produce potentially detectable SO_2 emissions (Table 4). Note that eruptions prior to 2004 were measured by the Total Ozone Mapping Spectrometer (TOMS) instruments, which had much lower sensitivity than OMI, OMPS and TROPOMI [*Carn et al.*, 2016]. Also, no TOMS instrument was operating in June 1995, when another submarine eruption occurred at Lateiki (Tonga) [*Global Volcanism Program*, 2013]. Table 4 includes two prior eruptions of HTHH in 2009 and 2014-15, which produced lower tropospheric plumes. One of the more remarkable events in Table 4 was the May 2010 eruption of South Sarigan seamount (CNMI), which produced a subaerial eruption column that rose to ~12 km from an eruption vent at ~200 m water depth [*Green et al*., 2013; *Searcy*, 2013; *Embley et al.* 2014]. To date, this appears to be the deepest submarine eruption to have produced SO_2 emissions detectable from space, although the measured SO_2 mass was low (~1 kiloton [kt]). Indeed, in a review of subaqueous eruptions, *Mastin and Witter* [2000] list only two other submarine volcanoes reported to have produced surface breaching from depths of >100 m: at Kick'em Jenny (West Indies) in 1939, 1974 and 1988; and Ritter Island (Papua New Guinea) in 1972 and 1974. In these cases the subaerial eruption columns extended only a few hundred meters above the ocean surface [*Mastin and Witter*, 2000]. Nevertheless, the 2010 South Sarigan eruption showed that unpredictable, upper tropospheric plumes are a potential hazard of submarine eruptions, and the January 2022 HTHH eruptions demonstrate that in rare cases such plumes can penetrate deep into the stratosphere.

The data in Table 4 suggest that, despite the potential for upper tropospheric or stratospheric plumes, SO_2 emissions from submarine eruptions are typically lower than subaerial eruptions of comparable magnitude (i.e., generating similar plume heights). This is likely due to the significant scrubbing of SO_2 expected in water-rich, submarine eruption plumes. The January 15, 2022 HTHH eruption produced the highest SO_2 emissions measured during a submarine eruption to date (~0.4-0.5 Tg), and yet the SO_2 mass is relatively modest given the inferred magnitude of the event (VEI 5-6). The mean SO_2 yield for magmatic eruptions with VEI 5 is ~2.3

Tg [*Carn et al.*, 2016], although there have been only 5 eruptions of this magnitude in the satellite era. Based on the data in Table 4, reduced SO_2 yield may be a consistent feature of submarine eruptions, with implications for their climate impacts, and making it difficult to assess the magnitude of such events based on SO_2 emissions alone.

As alluded to earlier, it is also apparent from Table 4 that the SO_2 emissions from HTHH in 2021-2022 were at least an order of magnitude higher than those measured during its previous eruptions in 2009 (0.0005 Tg SO_2) and 2014-2015 (0.014 Tg SO_2). This may be due in part to increasingly 'emergent' (i.e., subaerial) activity since 2009, with higher SO_2 fluxes due to reduced scrubbing of SO_2. Of particular significance is the period of continuous eruptive activity at HTHH between December 2021 and early January 2022 (~0.12 Tg SO_2), which in retrospect is a strong indication of a rejuvenated magmatic system prior to the January 13 and 15 eruptions. Although this may not represent a true eruption 'precursor', it was a much clearer manifestation of increased unrest than typically seen prior to submarine eruptions; e.g., before the 2019 Lateiki submarine eruption the only precursor was an 8-month non-unique increase in hydrothermal discharge [*Yeo et al.*, 2022].

6.2. Modest SO_2 emissions in the January 15, 2022 eruption

Although the precise eruption magnitude and erupted volume remain uncertain, the January 15, 2022 HTHH eruption undoubtedly rivals the largest eruptions of the past Century or more. The maximum plume height of ~55 km for the overshooting tops [*Carr et al.*, 2022] is unprecedented in the satellite era, *Wright et al.* [2022] estimate an eruption energy yield of 10-28 Exajoules (EJ; 1 EJ =10^{18} J), and *Matoza et al.* [2022] report exceptional atmospheric Lamb wave amplitudes. Based on these metrics, the climactic January 15, 2022 HTHH explosion was likely larger than the

1991 Pinatubo eruption and comparable to the 1883 Krakatau eruption. However, the HTHH SO_2 discharge (~0.4-0.5 Tg) is ~2 orders of magnitude lower than those eruptions, which produced ~15-30 Tg SO_2.

Although a detailed analysis is beyond the scope of this paper, there are several plausible reasons for the modest measured SO_2 emission. The January 15 HTHH eruption emitted at least ~150 Tg of water vapor [*Millán et al.*, 2022], likely dominated by evaporated seawater but potentially also including water vapor exsolved from magma and entrained from the atmosphere. Potentially significant amounts of SO_2 (and other soluble volcanic gases such as HCl) could have been scavenged by liquid water and ice particles in the water-rich HTHH plume [e.g., *Textor et al.*, 2003]. The DSCOVR/EPIC observations of the January 13 eruption (Section 5.3) are consistent with SO_2 scavenging by water, and this was perhaps even more efficient in the January 15 plume. Aura/MLS measured only a weak enhancement in stratospheric HCl on January 16-18 [*Millán et al.*, 2022], which is also consistent with scavenging by water. Other satellite observations of the January 15 HTHH eruption show large stratospheric aerosol optical depths (AODs) soon after the event, attributed to rapid sulfate aerosol formation [*Sellitto et al.*, 2022], which is another sink for SO_2. It is also possible that the magma driving the eruption was relatively sulfur-poor, or that sulfur outgassing was hindered by premature quenching of fragmented magma before complete vesiculation, which is a feature of Surtseyan eruptions [e.g., *Colombier et al.,* 2018]. Finally, it is well-known that magma-water interaction in phreatomagmatic eruptions can generate 1-2 orders of magnitude greater explosion energy than magmatic eruptions [e.g., *Sato and Taniguchi*, 1996]. Hence the magma mass supplying the HTHH eruption (i.e., the source of the emitted sulfur) could have been smaller than that erupted at Pinatubo or Krakatau, and yet could still have produced an explosion of comparable or larger size if magma-water interaction was highly efficient.

6.3. Water vapor emissions

Regardless of the origin of the modest SO_2 emissions, by far the most significant atmospheric impact of the January 15 HTHH eruption is likely to be the resulting stratospheric water vapor (SWV) injection [*Millán et al.*, 2022], which is also the probable cause of the short SO_2 lifetime (Fig. 5) [*Glaze et al.*, 1997; *Zhu et al.*, 2022], and will likely impact the stratospheric aerosol evolution in significant ways, e.g., by increasing aerosol size and AOD [*LeGrande et al.*, 2016]. *Millán et al.* [2022] estimate a SWV loading of 146±5Tg using Aura/MLS data (~10 % of the typical stratospheric water vapor burden), but the initial water vapor injection during the January 15 eruption could have been significantly higher due to early water loss to ice in the eruption plume [*Guo et al.*, 2004; *Zhu et al.*, 2022]. It is worth noting that the emission of ~150 Tg H_2O by a volcanic eruption would not be unprecedented; using petrological arguments, *Gerlach et al.* [1996] estimated that the 1991 Pinatubo eruption emitted ~500 Tg H_2O (derived from magmatic degassing and an accumulated vapor phase), although no SWV anomaly was measured after the eruption. *Guo et al.* [2004] also measured an additional ~80 Tg of ice in the young Pinatubo volcanic cloud. However, the HTHH SWV anomaly is unprecedented in its altitude (~25-30 km), and MLS H_2O measurements are the most effective way of tracking the zonal and meridional dispersion of the volcanic WV as it disperses in the stratosphere (Fig. 6).

Volcanic eruptions can increase SWV either by direct injection (as at HTHH), or by heating of the cold-point tropopause by volcanic aerosols, which increases the flux of tropospheric water vapor into the stratosphere [*Kroll et al.*, 2021]. Work by *Glaze et al.* [1997] on volcanic water vapor injection into the stratosphere found that larger eruption columns are dominated by magmatic water (not entrained atmospheric water), but they did not consider submarine eruptions. Based on modeling by *Glaze et al.* [1997], a large explosive eruption column in a wet atmosphere could inject ~4x10^9 kg WV per hour (4 Tg/hr); hence ~24 hours of continuous activity could deposit ~100 Tg WV into the stratosphere (equivalent to ~100 midlatitude thunderstorms or 7% of the total stratospheric WV). The January 2022 HTHH eruption injected at least as much WV in a shorter timespan (~11 hours).

Actual measurements of stratospheric volcanic WV injections are rare, and upper tropospheric volcanic WV injections are challenging to detect due to swamping by ambient tropospheric WV. Using Aura/MLS data, *Sioris et al*. [2016] estimated a SWV injection of ~2 Tg H_2O by the 2015 Calbuco (Chile) eruption (VEI 4), which was similar to short-lived (~1 week), local SWV perturbations observed after the 1980 Mount St. Helens (MSH) and 2008 Kasatochi eruptions. *Murcray et al.* [1981] measured up to ~40 ppm H_2O in the 1980 MSH eruption plume on May 22, 1980 at ~19-20 km altitude, against a background of 20-30 ppm. There are no in-situ SWV observations for the largest eruptions of recent decades (1982 El Chichón, 1991 Pinatubo, 1991 Cerro Hudson) although, as noted by *Glaze et al*. [1997], *Burnett and Burnett* [1984] reported elevated OH radicals after the 1982 El Chichón eruption, possibly sourced from the volcanic WV injection. Based on petrological estimates, the 1815 Tambora eruption (VEI 7) could have injected up to 2000-3000 Tg WV into the stratosphere, which would double the stratospheric WV load [*Glaze et al.*, 1997]. For the ~75 ka Toba eruption, the WV injection could have been on the order of 27 Pg (27000 Tg) [*LeGrande et al.*, 2016]. However, the 2022 HTHH ~150 Tg SWV injection is clearly the largest such perturbation measured in the instrumental era, revealing that submarine volcanic eruptions may be a previously unrecognized, yet effective (though perhaps rare) mechanism for stratospheric hydration.

6.4. Optical effects of the stratospheric volcanic cloud

Another measure of eruption magnitude and atmospheric impact is the geographical extent of the resulting atmospheric optical effects. The January 15, 2022 HTHH eruption is perhaps the largest volcanic explosion since the 1883 Krakatau eruption, and the vivid volcanic twilights, 'blue suns and moons' and other atmospheric phenomena observed in the months after August 1883 are well known [*Symons et al.*, 1888]. However, given the modest HTHH SO_2 emission (~1-2 orders of magnitude less than Krakatau and Pinatubo) and the high SWV loading, we might expect different effects in 2022 due to the distinctive stratospheric aerosol composition (fewer primary sulfate particles) and probable larger 'hydrated' aerosol particle size [e.g., *Zhu et al.*, 2022; *Sellitto et al.*, 2022]. To date, this appears consistent with limited atmospheric observations from the southern hemisphere (e.g., public photos from Australia, Zimbabwe and Chile posted on the Space Weather image gallery: https://spaceweathergallery.com/index.php).

There have been no reports of blue (or otherwise unusually colored) suns or moons since the HTHH eruption, but these were observed soon (a few days to weeks) after the August 1883 Krakatau eruption [*Symons et al.*, 1888]. Since 'blueing' of the Sun or Moon requires a specific stratospheric aerosol particle size of ~0.5 µm [e.g., *Garrison et al.*, 2021], this may tentatively be attributed to the larger size of the HTHH aerosol particles. Another atmospheric phenomenon first reported after the 1883 Krakatau eruption was the 'Bishop's Ring' halo around the Sun, observed from Honolulu (Hawai'i) by the Reverend Sereno Bishop [*Hamilton*, 2012]. A similar solar halo was observed from Zimbabwe (at a similar latitude to Tonga) throughout the day on February 12, 2022 (https://spaceweathergallery.com/indiv_upload.php?upload_id=182436). Aerosols or ice crystals at very high altitudes near the mesopause can also form noctilucent clouds, and such clouds have been observed in the aftermath of the HTHH eruption, such as this example from Chile on January 30, 2022: https://spaceweathergallery.com/indiv_upload.php?upload_id=182031. As indicated by the SWV distribution in Figure 6, the HTHH stratospheric aerosol and WV veil has not penetrated deep into the northern hemisphere to date, but in the coming months we might expect more atmospheric optical effects to be reported from further north as the aerosols are dispersed meridionally by the Brewer-Dobson Circulation.

The initial dispersion of the January 15 HTHH eruption cloud also bore a strong resemblance to the 1883 Krakatau eruption. After the 1883 eruption, the Krakatau volcanic aerosol cloud (and associated twilight phenomena) spread rapidly westwards from Indonesia and completed a global circuit in ~2 weeks [*Hamilton*, 2012]. The 1883 eruption provided the first observation of tropical stratospheric winds (the 'Krakatoa Easterlies') and was key to the later discovery of the phased variability in stratospheric wind direction now known as the Quasi-biennial Oscillation (QBO) [*Hamilton*, 2012; Fig. 6]. Similarly, after the January 15, 2022 HTHH eruption, the high-level SWV anomaly at 2.1 hPa (~45 km altitude) dispersed rapidly west under the prevailing easterly phase of the QBO, and had almost entirely circled the globe by January 22, whilst SWV at lower altitudes (26 hPa) traveled more slowly [*Millán et al.*, 2022].

6.5. Challenges for eruption response, volcanic cloud sampling and tracking

NASA has a major volcanic eruption response plan to activate in the event of a major explosive eruption that could potentially impact climate [e.g., *Carn et al.*, 2021]. However, the 2022 HTHH eruption was unexpected in its magnitude and plume altitude (~30-55 km) and posed unanticipated challenges for volcanic cloud sampling and eruption response (e.g., in-situ sampling). The ~30 km altitude of the January 15 HTHH umbrella cloud, at which most emissions (WV, SO_2) were emplaced, is too high for direct sampling by NASA's high-altitude aircraft (e.g., NASA's ER-2 has a ceiling of ~21 km altitude), and hence direct sampling of the stratospheric volcanic gas and aerosol cloud must rely on balloon-borne campaigns [e.g., *Kloss et al.*, 2022]. Furthermore, the modest HTHH SO_2 loading (but high WV loading) defies conventional views of climate-forcing eruptions, since the NASA eruption response is based primarily upon high SO_2 loading measured by satellites (where >5 Tg SO_2 indicates a potentially significant event), whereas in the HTHH case the SWV anomaly is the more significant effect, and could lead to surface warming rather than the cooling expected after SO_2-rich stratospheric eruptions [e.g., *Joshi and Jones*, 2009; *Sellitto et al.*, 2022; *Millán et al.*, 2022].

The 2022 HTHH eruption also comes at a turning point in NASA's satellite observation strategy. The agency plans to terminate its Earth Observing System flagship Terra (1999 – present), Aqua (2002 – present) and Aura (2004 - present) missions in summer 2023 to prepare for the next generation Earth System Observatory (https://science.nasa.gov/earth-science/earth-system-observatory), although the Aura mission has sufficient fuel and solar power generation to continue operating until 2025. Termination of Aura would mean the loss of OMI SO_2 and MLS H_2O measurements, which would preclude monitoring of the unprecedented HTHH SWV anomaly (Fig. 6), which could persist for several years and have significant impacts on stratospheric chemistry (e.g., ozone depletion) and climate. The historic HTHH eruption therefore constitutes strong motivation for extending the Aura mission for as long as spacecraft resources permit.

6. Summary

The January 15, 2022 HTHH eruption ranks among the largest volcanic eruptions since 1883, but UV satellite observations from OMI, OMPS, TROPOMI and EPIC indicate a modest stratospheric SO_2 injection of ~0.4-0.5 Tg, consistent with other satellite measurements. A month of Surtseyan eruptive activity and precursory explosive eruptions (December 2021 – January 2022) emitted an additional ~0.2 Tg SO_2, significantly exceeding SO_2 emissions from prior HTHH eruptions and providing strong evidence for rejuvenation of the HTHH volcanic system prior to the paroxysmal event. The relatively low SO_2 loading and short stratospheric SO_2 lifetime observed after the 2022 HTHH eruptions are most likely attributed to abundant WV in the volcanic plumes, which also has implications for the evolution and impacts of the stratospheric aerosols and the related optical effects.

Acknowledgements

We acknowledge funding from the NASA Earth Science Division through the Science of Terra, Aqua and SNPP (grant 80NSSC18K0688), Aura Science Team (grant 80NSSC20K0983), DSCOVR Science Team (grant 80NSSC19K0771) and Interdisciplinary Research in Earth Science (grant 80NSSC20K1773) programs.

References

Burnett, C. R., and E. B. Burnett (1984), Observational results on the vertical column abundance of atmospheric hydroxyl: Description of its seasonal behavior 1977-1982 and of the 1982 E1 Chichón perturbation, *J. Geophys Res*., 89, 9603-9611.

Cahalan, R. C., and J. Dufek (2021), Explosive submarine eruptions: The role of condensable gas jets in underwater eruptions. *J. Geophys Res*, 126, e2020JB020969, https://doi.org/10.1029/2020JB020969.

Carn, S.A. (2022), Multi-Satellite Volcanic Sulfur Dioxide L4 Long-Term Global Database V4, Greenbelt, MD, USA, Goddard Earth Science Data and Information Services Center (GES DISC), Accessed: 14 April 2022, doi:10.5067/MEASURES/SO2/DATA405.

Carn, S.A., K. Yang, A.J. Prata, and N.A. Krotkov (2015), Extending the long-term record of volcanic SO_2 emissions with the Ozone Mapping and Profiler Suite (OMPS) Nadir Mapper, *Geophys. Res. Lett*., 42, 925-932, doi: 10.1002/2014GL062437.

Carn, S.A., L. Clarisse and A.J. Prata (2016), Multi-decadal satellite measurements of global volcanic degassing, *J. Volcanol. Geotherm. Res*., 311, 99-134, http://dx.doi.org/10.1016/j.jvolgeores.2016.01.002.

Carn, S.A., N.A. Krotkov, B.A. Fisher, C. Li, and A.J. Prata (2018), First observations of volcanic eruption clouds from the L1 Earth-Sun Lagrange point by DSCOVR/EPIC, *Geophys. Res. Lett*., 45. https://doi.org/10.1029/2018GL079808.

Carn, S.A., P.A. Newman, V. Aquila, H. Gonnermann, and J. Dufek (2021), Preparing NASA for the next major volcanic eruption, *Eos*, 102, https://doi.org/10.1029/2021EO162730.

Carr, J.L., Á. Horváth, D.L. Wu, and M.D. Friberg (2022), Stereo plume height and motion retrievals for the record-setting Hunga Tonga- Hunga Ha'apai eruption of 15 January 2022. *Geophys. Res. Lett.*, 49, e2022GL098131. https://doi. org/10.1029/2022GL098131.

Colombier, M., B. Scheu, F.B. Wadsworth, S. Cronin, J. Vasseur, K.J. Dobson, et al. (2018). Vesiculation and quenching during Surtseyan eruptions at Hunga Tonga-Hunga Ha'apai volcano, Tonga. *J. Geophys. Res.*, 123, 3762–3779. https://doi.org/10.1029/2017JB015357.

Constantinescu, R., A. Hopulele-Gligor, C.B. Connor, et al. (2021), The radius of the umbrella cloud helps characterize large explosive volcanic eruptions. *Commun Earth Environ* 2, 3, https://doi.org/10.1038/s43247-020-00078-3.

Cronin, S. J.,Brenna, M.,Smith, I. E. M.,Barker, S. J.,Tost, M.,Ford, M.,Tonga'onevai, S.,Kula, T., and Vaiomounga, R. (2017), New volcanic island unveils explosive past, *Eos*, 98, https://doi.org/10.1029/2017EO076589.

Embley, R.W., Y. Tamura, S.G. Merle, T. Sato, O. Ishizuka, W.W. Chadwick Jr., D.A. Wiens, P. Shore, and R.J. Stern (2014). Eruption of South Sarigan Seamount, Northern Mariana Islands: Insights into hazards from submarine volcanic eruptions. *Oceanography* 27(2):24–31, http://dx.doi.org/10.5670/oceanog.2014.37.

Fisher, B.L., N.A. Krotkov, P.K. Bhartia, C. Li, S.A. Carn, E. Hughes, and P.J.T. Leonard (2019), A new discrete wavelength backscattered ultraviolet algorithm for consistent volcanic SO_2 retrievals from multiple satellite missions, *Atmos. Meas. Tech.*, 12, 5137-5153, https://doi.org/10.5194/amt-12-5137-2019.

Garrison, C., C. Kilburn, D. Smart, and S. Edwards (2021), The blue suns of 1831: was the eruption of Ferdinandea, near Sicily, one of the largest volcanic climate forcing events of the nineteenth century?, *Clim. Past*, 17, 2607–2632, https://doi.org/10.5194/cp-17-2607-2021.

Garvin, J. B., D.A. Slayback, V. Ferrini, J. Frawley, C. Giguere, G.R. Asrar, and K. Andersen (2018). Monitoring and modeling the rapid evolution of Earth's newest volcanic island: Hunga Tonga Hunga Ha'apai (Tonga) using high spatial resolution satellite observations. *Geophys. Res. Lett*, 45, 3445–3452. https://doi.org/10.1002/ 2017GL076621.

Gerlach, T.M., H.R. Westrich, and R.B. Symonds (1996), Preeruption vapor in magma of the climactic Mount Pinatubo eruption: source of the giant stratospheric sulfur dioxide cloud. In: Newhall, C.G., Punongbayan, R.S. (Eds.), Fire and Mud: Eruptions and Lahars of Mount Pinatubo, Philippines. University of Washington Press, Seattle, USA, pp. 415–434; https://pubs.usgs.gov/pinatubo/index.html.

Glaze, L.S., S.M. Baloga, L. Wilson (1997), Transport of atmospheric water vapor by volcanic eruption columns, *J. Geophys. Res.*, 102(D5), 6099-6108.

Global Volcanism Program, 2013. Volcanoes of the World, v. 4.10.6 (24 Mar 2022). Venzke, E (ed.). Smithsonian Institution. Downloaded 05 Apr 2022. https://doi.org/10.5479/si.GVP.VOTW4-2013.

Global Volcanism Program, 2021a. Report on Hunga Tonga-Hunga Ha'apai (Tonga). In: Sennert, S K (ed.), Weekly Volcanic Activity Report, 15 December-21 December 2021. Smithsonian Institution and US Geological Survey.

Global Volcanism Program, 2021b. Report on Hunga Tonga-Hunga Ha'apai (Tonga). In: Sennert, S K (ed.), Weekly Volcanic Activity Report, 22 December-28 December 2021. Smithsonian Institution and US Geological Survey.

Global Volcanism Program, 2021c. Report on Hunga Tonga-Hunga Ha'apai (Tonga). In: Sennert, S K (ed.), Weekly Volcanic Activity Report, 29 December-4 January 2022. Smithsonian Institution and US Geological Survey.

Global Volcanism Program, 2022. Report on Hunga Tonga-Hunga Ha'apai (Tonga). In: Sennert, S K (ed.), Weekly Volcanic Activity Report, 12 January-18 January 2022. Smithsonian Institution and US Geological Survey.

Green, D.N., L.G. Evers, D. Fee, R.S. Matoza, M. Snellen, P. Smets, and D. Simons (2013), Hydroacoustic, infrasonic and seismic monitoring of the submarine eruptive activity and sub-aerial plume generation at South Sarigan, May 2010, *J. Volcanol. Geotherm. Res*., 257, 31-43, https://doi.org/10.1016/j.jvolgeores.2013.03.006.

Guo, S., W.I. Rose, G.J.S. Bluth, and I.M. Watson (2004), Particles in the great Pinatubo volcanic cloud of June 1991: The role of ice. *Geochemistry, Geophysics, Geosystems* 5, Q05003, doi:10.1029/2003GC000655.

Hamilton, K. (2012), Sereno Bishop, Rollo Russell, Bishop's Ring and the Discovery of the “Krakatoa Easterlies”, *Atmosphere-Ocean*, 50:2, 169-175, doi:10.1080/07055900.2011.639736.

Herman, J., Huang, L., McPeters, R., Ziemke, J., Cede, A., & Blank, K. (2018), Synoptic ozone, cloud reflectivity, and erythemal irradiance from sunrise to sunset for the whole Earth as viewed by the DSCOVR spacecraft from the Earth-Sun Lagrange 1 orbit. *Atmos. Meas. Tech,* 11(1), 177–194. https://doi.org/10.5194/amt-11-177-2018.

Joshi, M. M., and G.S. Jones (2009), The climatic effects of the direct injection of water vapour into the stratosphere by large volcanic eruptions. *Atmos. Chem. Phys.*, 9(16), 6109–6118, https://doi.org/10.5194/acp-9-6109-2009.

Kloss, C., P. Sellitto, J.-B. Renard, et al. (2022), Aerosol characterization of the stratospheric plume from the volcanic eruption at Hunga Tonga January 15th 2022, *Earth and Space Science Open Archive*, https://doi.org/10.1002/essoar.10511312.1.

Kroll, C. A., Dacie, S., Azoulay, A., Schmidt, H., and Timmreck, C. (2021), The impact of volcanic eruptions of different magnitude on stratospheric water vapor in the tropics, *Atmos. Chem. Phys*., 21, 6565–6591, https://doi.org/10.5194/acp-21-6565-2021.

Kubota, T., T. Saito, and K. Nishida (2022), Global fast-traveling tsunamis driven by atmospheric Lamb waves on the 2022 Tonga eruption, *Science*, 10.1126/science.abo4364.

LeGrande, A. N., Tsigaridis, K., and Bauer, S. E. (2016). Role of Atmospheric Chemistry in the Climate Impacts of Stratospheric Volcanic Injections. *Nat. Geosci*. 9, 652–655. doi:10.1038/ngeo2771.

Levelt, P., et al. (2018), The Ozone Monitoring Instrument: Overview of 14 years in space, *Atmos. Chem. Phys*., 18, 5699-5745, https://doi.org/10.5194/acp-18-5699-2018.

Li, C., N.A. Krotkov, S.A. Carn, Y. Zhang, R.J.D. Spurr, and J. Joiner (2017), New-generation NASA Aura Ozone Monitoring Instrument volcanic SO_2 dataset: Algorithm description, initial results, and continuation with the Suomi-NPP Ozone Mapping and Profiler Suite, *Atmos. Meas. Tech*., 10, 445-458, doi:10.5194/amt-10-445-2017.

Lopez, T., Clarisse, L., Schwaiger, H. et al. (2020), Constraints on eruption processes and event masses for the 2016–2017 eruption of Bogoslof volcano, Alaska, through evaluation of IASI satellite SO_2 masses and complementary datasets. *Bull. Volcanol.* 82, 17, https://doi.org/10.1007/s00445-019-1348-z.

Marshak, A., J. Herman, A. Szabo, K. Blank, A. Cede, S. Carn, I. Geogdzhayev, D. Huang, L.-K. Huang, Y. Knyazikhin, M. Kowalewski, N. Krotkov, A. Lyapustin, R. McPeters, O. Torres, and Y. Yang (2018), Earth observations from DSCOVR/EPIC instrument, *Bull. Amer. Meteor. Soc.*, 99(9), 1829-1850, doi:10.1175/BAMS-D-17-0223.1.

Mastin, L.G., and J.B. Witter (2000), The hazards of eruptions through lakes and seawater. *J. Volcanol. Geotherm. Res.*, 97, 195–214, http://dx.doi.org/10.1016/S03770273(99)00174-2.

Matoza, R.S., et al. (2022), Atmospheric waves and global seismoacoustic observations of the January 2022 Hunga eruption, Tonga, *Science*, 10.1126/science.abo7063.

Millán, L. et al. (2022), Hunga Tonga-Hunga Ha'apai Hydration of the Stratosphere. Preprint ESSOAr, doi:doi.org/10.1002/essoar.10511266.1.

Murcray, D.G., F.J. Murcray, D.B. Barker, and H.J. Mastenbrook (1981), Changes in stratospheric water vapor associated with the Mount St. Helens eruption, *Science*, 211, 823–824, doi:10.1126/science.211.4484.823.

Prata, A.T., Folch, A., Prata, A.J. et al. (2020), Anak Krakatau triggers volcanic freezer in the upper troposphere. *Sci. Rep.* 10, 3584, https://doi.org/10.1038/s41598-020-60465-w.

Searcy, C. (2013), Seismicity Associated with the May 2010 Eruption of South Sarigan Seamount, Northern Mariana Islands. *Seismological Research Letters*, 84(6), 1055–1061, doi: 10.1785/0220120168.

Sellitto, P., A. Podglajen, R. Belhadji et al. (2022), The unexpected radiative impact of the Hunga Tonga eruption of January 15th, 2022, 18 April 2022, PREPRINT (Version 1) available at Research Square, https://doi.org/10.21203/rs.3.rs-1562573/v1.

Sioris, C. E., A. Malo, C. A. McLinden, and R. D'Amours (2016), Direct injection of water vapor into the stratosphere by volcanic eruptions, *Geophys. Res. Lett.*, 43, 7694–7700, doi:10.1002/ 2016GL069918.

Suzuki, Y. J., and T. Koyaguchi (2009), A three-dimensional numerical simulation of spreading umbrella clouds, *J. Geophys. Res*., 114, B03209, doi:10.1029/2007JB005369.

Symons, G.J. (ed.), 1888. The Eruption of Krakatoa, and subsequent phenomena. Report of the Krakatoa Committee of the Royal Society. Royal Society, London, U.K.

Textor, C., H.-F. Graf, M. Herzog, and J. M. Oberhuber (2003), Injection of gases into the stratosphere by explosive volcanic eruptions, *J. Geophys. Res*., 108(D19), 4606, doi:10.1029/2002JD002987.

Theys, N. et al. (2017), Sulfur dioxide retrievals from TROPOMI onboard Sentinel-5 Precursor: algorithm theoretical basis. *Atmos. Meas. Tech*. 10, 119–153, https://doi.org/10.5194/amt-10-119-2017.

Van Eaton, A.R., Á. Amigo, D. Bertin, L.G. Mastin, R.E. Giacosa, J. González, O. Valderrama, K. Fontijn, and S.A. Behnke (2016), Volcanic lightning and plume behavior reveal evolving hazards during the April 2015 eruption of Calbuco volcano, Chile, *Geophys. Res. Lett*., 43, doi:10.1002/2016GL068076.

Vaughan, R. G., & Webley, P. (2010). Satellite observations of a surtseyan eruption: Hunga Ha'apai, Tonga. *J. Volcanol. Geotherm. Res*., 198(1–2), 177–186. https://doi.org/10.1016/j.jvolgeores.2010.08.017.

Veefkind, J. P., et al. (2012), TROPOMI on the ESA Sentinel-5 Precursor: A GMES mission for global observations of the atmospheric composition for climate, air quality and ozone layer applications, *Remote Sens. Environ*., 120, 70–83, doi:10.1016/j.rse.2011.09.027.

Woods, A.W. and Kienle, J. (1994), The dynamics and thermodynamics of volcanic clouds: Theory and observations from the April 15 and April 21, 1990 eruptions of Redoubt volcano, Alaska. *J. Volcanol. Geotherm. Res*. 62, 273–299, https://doi.org/10.1016/0377-0273(94)90037-X.

Wright, C., et al. (2022). Tonga eruption triggered waves propagating globally from surface to edge of space, *Earth and Space Science Open Archive*, https://doi.org/10.1002/essoar.10510674.1.

Yeo, I.A., McIntosh, I.M., Bryan, S.E. et al. (2022), The 2019–2020 volcanic eruption of Late'iki (Metis Shoal), Tonga. *Sci. Rep.* 12, 7468, https://doi.org/10.1038/s41598-022-11133-8.

Zhu, Y., Toon, O.B., Jensen, E.J. et al. (2020), Persisting volcanic ash particles impact stratospheric SO_2 lifetime and aerosol optical properties. *Nat. Commun.* 11, 4526, https://doi.org/10.1038/s41467-020-18352-5.

Zhu, Y., C. Bardeen, S. Tilmes et al. (2022), 2022 Hunga-Tonga eruption: stratospheric aerosol evolution in a water-rich plume, Preprint (Version 1) available at Research Square https://doi.org/10.21203/rs.3.rs-1647643/v1.

Table 1. UV satellite instruments

Sensor	**Satellite**	**Spatial resolution (nadir, km)**	**Temporal resolution**	**SO_2 algorithm**
OMI	Aura	13 × 24	1 day	*Li et al.* (2017)
OMPS	Suomi-NPP	50 × 50	1 day	*Li et al.* (2017)
EPIC	DSCOVR	18 × 18	~110 min (daytime)	*Fisher et al.* (2019)
TROPOMI	S5P	7 × 3.5	1 day	*Theys et al*. (2017)

Table 2. Satellite measurements of SO_2 emissions from HTHH during the December 2021 – January 2022 eruption sequence

Date (UT)	Time (UT)	Satellite/sensor	SO_2 (Tg)	Plume height (km)[1]	Notes
Dec 19, 2021	**20:35**	**HTHH eruption**		**16**	
	20:53	DSCOVR/EPIC	0.0003		
	22:41	DSCOVR/EPIC	0.002		
Dec 20	01:25	Aura/OMI	0.01		
	02:00	SNPP/OMPS	0.01		
	02:03	S5P/TROPOMI	0.01		
Dec 21		SNPP/OMPS	0.002	6-12	Surtseyan activity
Dec 22		SNPP/OMPS	0.013	8-14	Surtseyan activity
Dec 23		SNPP/OMPS	0.015	6-11	Surtseyan activity
Dec 24		SNPP/OMPS	0.015	3-12	Surtseyan activity
Dec 25		SNPP/OMPS	0.013		Surtseyan activity
Dec 26		SNPP/OMPS	0.011		Surtseyan activity
Dec 27		SNPP/OMPS	0.011	3-16	Surtseyan activity
Dec 28		SNPP/OMPS	0.015	<12	Surtseyan activity
Dec 29		SNPP/OMPS	0.011	<12	Surtseyan activity
Dec 30		SNPP/OMPS	0.005	<12	Surtseyan activity
Dec 31		SNPP/OMPS	0.006	3-18	Surtseyan activity
Jan 1, 2022		SNPP/OMPS	0.006		Surtseyan activity
Jan 2		SNPP/OMPS			Surtseyan activity
Jan 3-6					*No SO_2 detected*
Jan 7		SNPP/OMPS	0.00		SO_2 degassing
Jan 8		S5P/TROPOMI	0.0005		SO_2 puff
Jan 9		S5P/TROPOMI	0.0001		SO_2 puff
Jan 10-12					*No SO_2 detected*
Jan 13, 2022	**15:20**	**HTHH Eruption**		**20**	
	19:56	DSCOVR/EPIC	0.019		
	21:44	DSCOVR/EPIC	0.011		
Jan 14	00:27	DSCOVR/EPIC	0.010		
	00:50	SNPP/OMPS	0.056		
	00:54	S5P/TROPOMI	0.053		
	01:18	Aura/OMI	0.058		
	02:15	DSCOVR/EPIC	0.009		Low sensitivity
	04:03	DSCOVR/EPIC	0.032		High SZA/VZA
	20:15	DSCOVR/EPIC	0.005		Partial coverage
Jan 15	02:12	SNPP/OMPS	0.059		
	02:16	S5P/TROPOMI	0.058		
Jan 15	**04:00**	**HTHH Eruption**		**30-55**	
	18:46	DSCOVR/EPIC	0.026		Partial coverage
	20:34	DSCOVR/EPIC	0.22		
	22:22	DSCOVR/EPIC	0.09		Partial coverage
Jan 16	01:53	SNPP/OMPS	0.42		
	01:57	S5P/TROPOMI	0.40		Partial coverage

Table 3. Growth of the January 13, 2022 HTHH volcanic SO_2 cloud observed by DSCOVR/EPIC and TROPOMI

Date (UT)	**Time (UT)**	**Time since eruption (min)**	**Plume area (km^2)**	**Equivalent radius (km)**	**Sensor**
Jan 13	19:56	264	104500	182	DSCOVR/EPIC
Jan 13	21:44	372	126000	200	DSCOVR/EPIC
Jan 14	00:27	535	261100	288	DSCOVR/EPIC
Jan 14	00:54	562	366600	341	S5P/TROPOMI

Table 4. Submarine volcanic eruptions in the satellite era (since 1978) with potential or confirmed subaerial plumes

Volcano	**Elevation (m)**[1]	**Eruption date(s)**	**SO_2 (kt)**[2]	**Plume height**[3]
Lateiki (Tonga)[4]	43	May-Jul 1979	nd	Pumice rafts
Home Reef (Tonga)	-10	Mar 1, 1984	nd	12
Fukutoku-Oka-no-Ba (Japan)	-29	Jan 20, 1986	5?	4?
Bogoslof (USA)	150	Jul 6, 1992	nd	6
Fukutoku-Oka-no-Ba (Japan)	-29	Jul 1, 2005	5?	1?
Home Reef (Tonga)	-10	Aug 8-15, 2006	~50	>5
HTHH (Tonga)	114	Mar 13, 2009	0.5	4 – 7.6*
South Sarigan (CNMI)	-184	May 29, 2010	1.1	12
HTHH (Tonga)	114	Dec 24, 2014	14	3
Bogoslof (USA)	150	Dec 2016-Aug 2017	0.1-22*	12*
Lateiki (Tonga)	43	Oct 13, 2019	0.2	3-5
Fukutoku-Oka-no-Ba (Japan)	-29	Aug 12, 2021	20	17
HTHH (Tonga)	114	Dec 20, 2021	10	16
HTHH (Tonga)	114	Jan 13, 2022	60	20
HTHH (Tonga)	114	Jan 15, 2022	400-500	30-55

1. Denotes the maximum elevation of each volcanic edifice above sea level. Although some volcanoes are partly emergent, all eruptions listed here are assumed to originate from submarine vents (depth usually unknown).
2. From *Carn* [2022]; nd: none detected above sensor detection limits (~5-10 kt).
3. Maximum reported volcanic plume height above sea level, as reported in the Smithsonian Institution Global Volcanism Program Volcanoes of the World database [*Global Volcanism Program*, 2013], unless otherwise noted. For some submarine eruptions (e.g., 1979 Lateiki), the only evidence of eruption is pumice rafts.
4. Lateiki was previously known as Metis Shoal.
* 2009 HTHH plume heights from *Vaughan and Webley* [2010]; 2016-2017 Bogoslof plume heights and SO_2 emissions from *Lopez et al.* [2020].

Figures

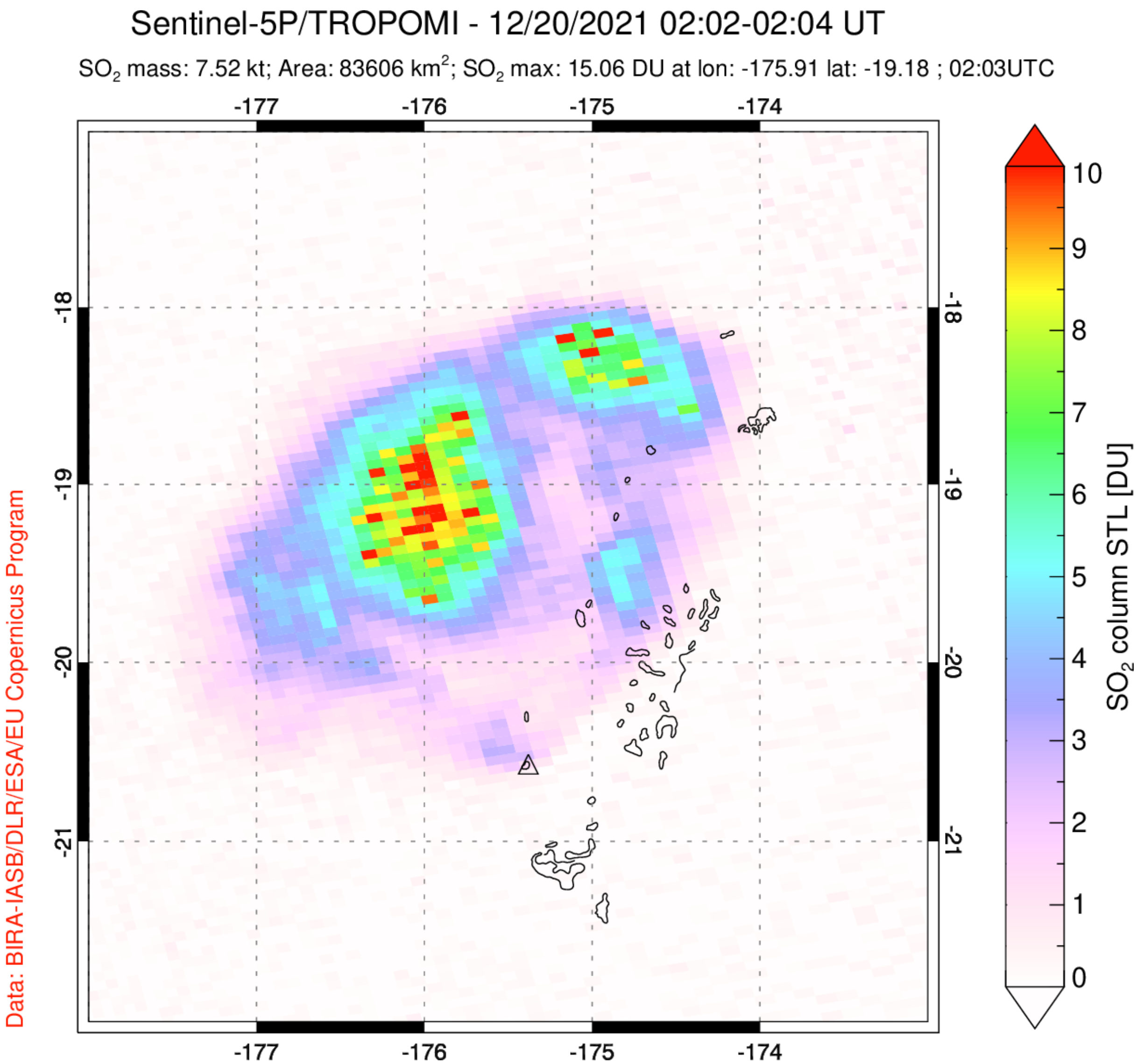

Figure 1. Lower stratospheric (STL) SO_2 columns measured by S5P/TROPOMI in the volcanic cloud produced by the eruption of HTHH at 20:35 UTC on December 19, 2021. The retrieved SO_2 columns (<10 DU) and the total SO_2 mass (8 kilotons; ~0.01 Tg) are both relatively low for a fresh, upper tropospheric volcanic cloud.

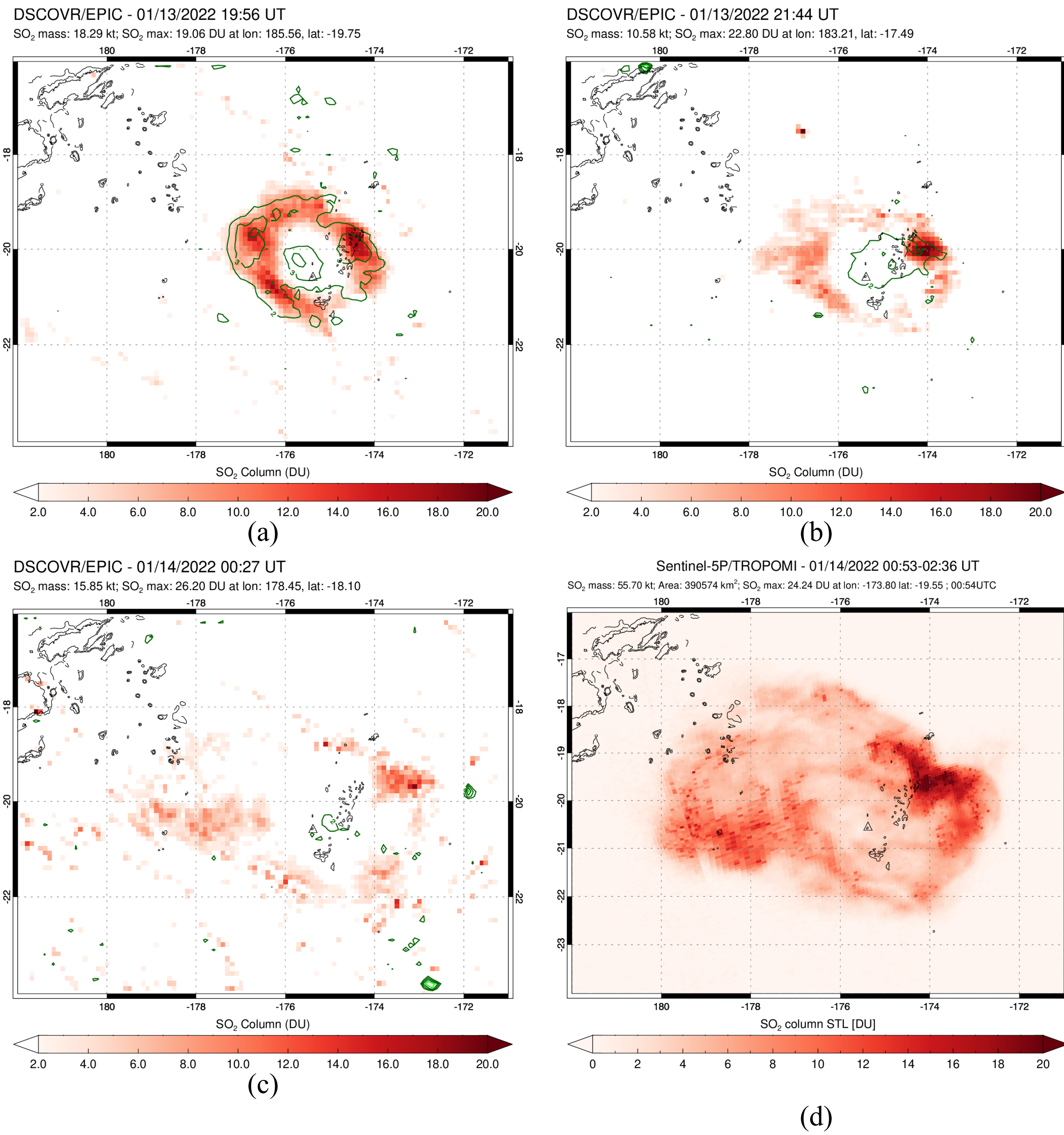

Figure 2. UV satellite observations of the January 13, 2022 HTHH volcanic SO_2 cloud by DSCOVR/EPIC and TROPOMI. *Green contours* in (a)-(c) show the EPIC UV Aerosol Index (UVAI), where positive values indicate absorbing aerosols such as volcanic ash (note low UVAI values in this case). (a) DSCOVR/EPIC SO_2 data at 19:56 UTC; (b) DSCOVR/EPIC SO_2 data at 21:44 UTC; (c) DSCOVR/EPIC SO_2 data at 00:27 UTC on January 14; (d) S5P/TROPOMI SO_2 data at 00:53 UTC on January 14.

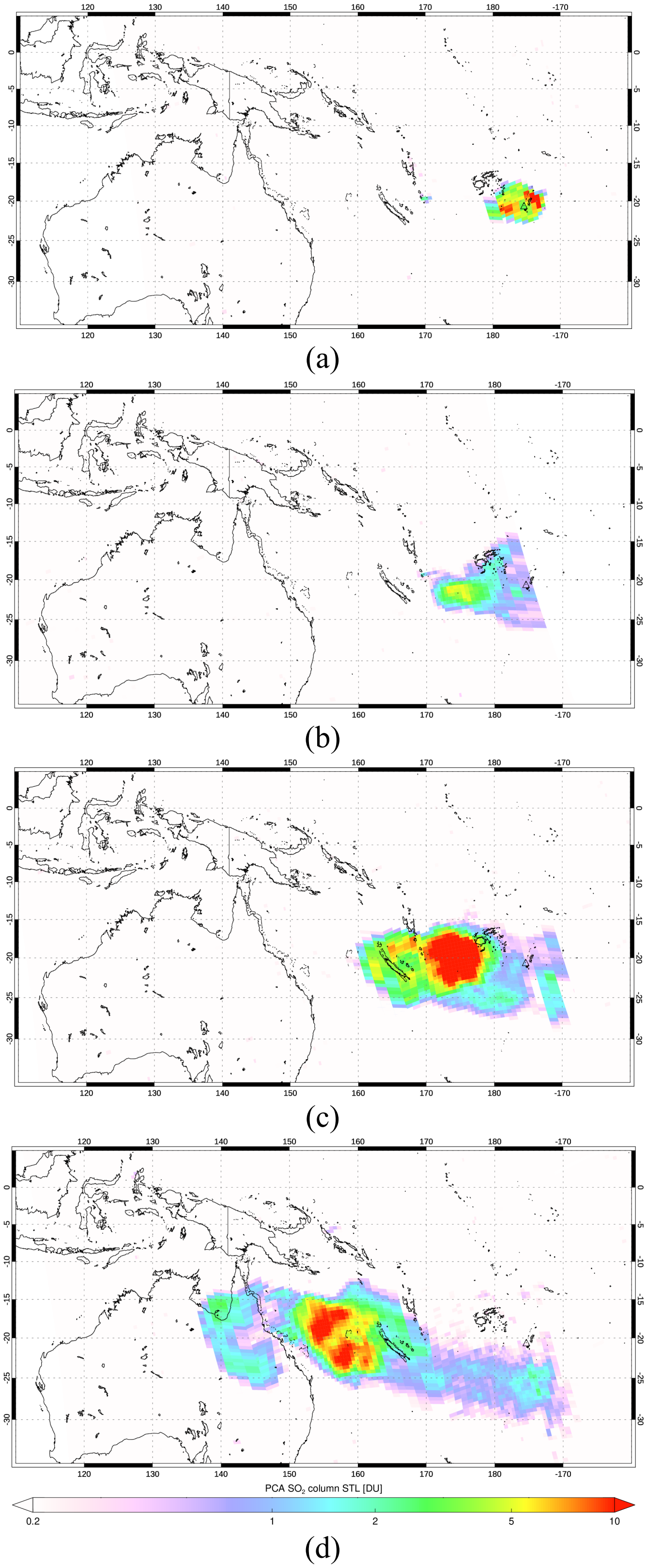

Figure 3. Daily SNPP/OMPS observations of HTHH SO_2 emissions from January 14-17, 2022. (a) 00:50 UTC on Jan 14 (0.06 Tg SO_2); (b) 02:12 UTC on Jan 15 (0.06 Tg SO_2); (c) 01:53 UTC on Jan 16 (0.4 Tg SO_2); (d) 03:16 UTC on Jan 17 (0.38 Tg SO_2).

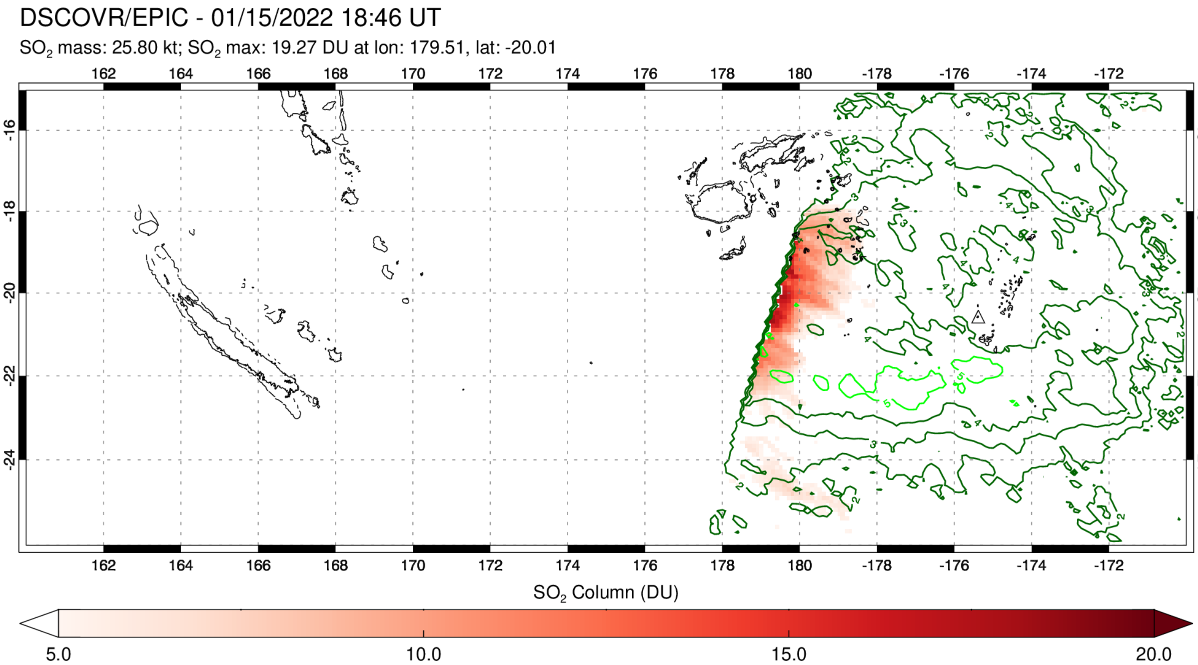

(a)

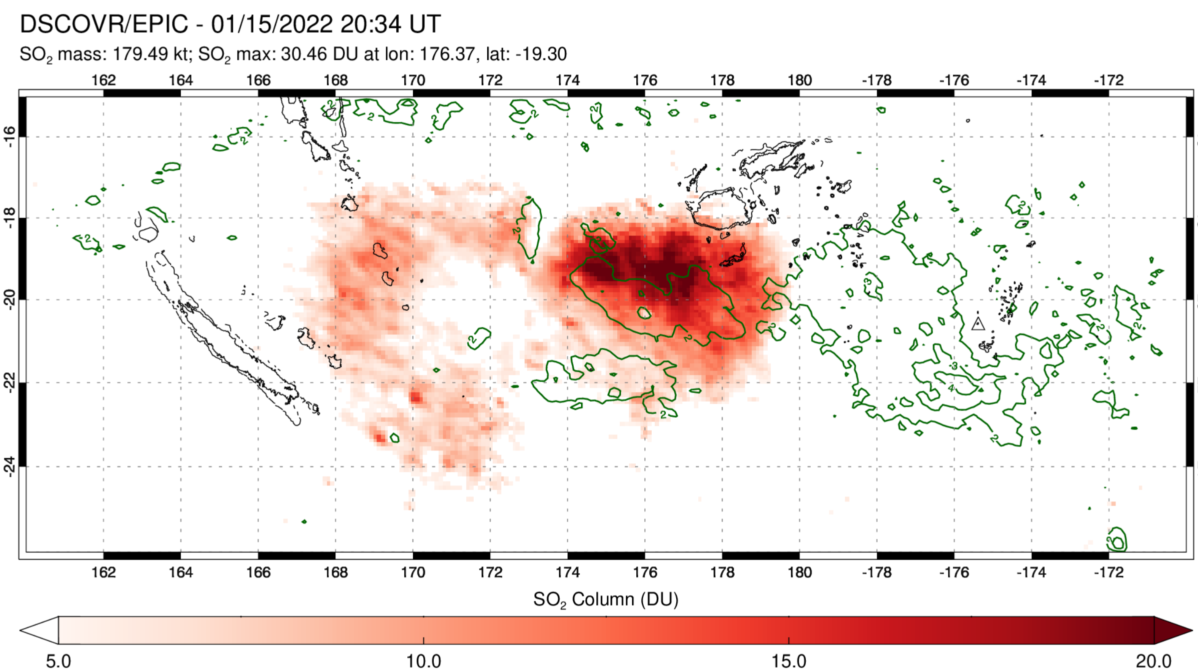

(b)

Figure 4. DSCOVR/EPIC observations of the January 15, 2022, HTHH eruption cloud. *Green contours* show the EPIC UV Aerosol Index (UVAI), where positive values indicate absorbing aerosols such as volcanic ash (but note low UVAI values in this case). (a) Detection of the eastern edge of the plume at 18:46 UTC on Jan 15; (b) Full coverage of the volcanic SO_2 cloud at 20:34 UTC on January 15. Note the ~200 km westward drift of the SO_2 cloud in the 108 minutes between the two EPIC exposures.

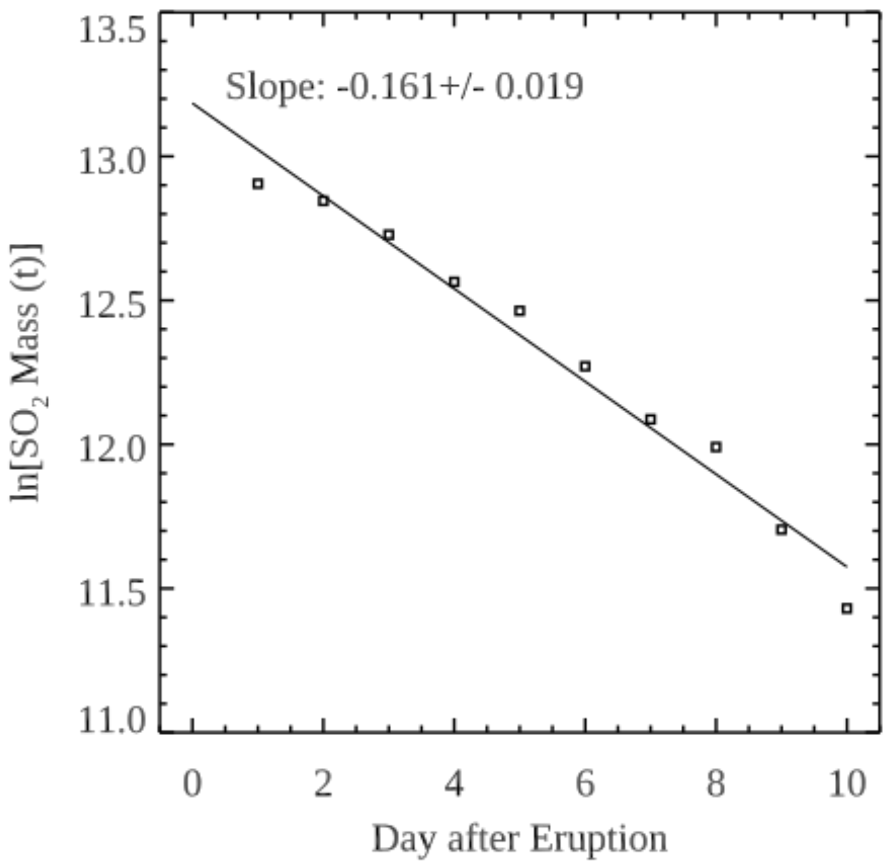

Figure 5. Trend in SO_2 mass measured by SNPP/OMPS in the January 15, 2022 HTHH eruption cloud during 10 days of atmospheric residence. The SO_2 mass e-folding time is ~6 days, and extrapolation of the SO_2 mass decay back to the eruption time yields an estimated initial SO_2 mass of 0.54 Tg.

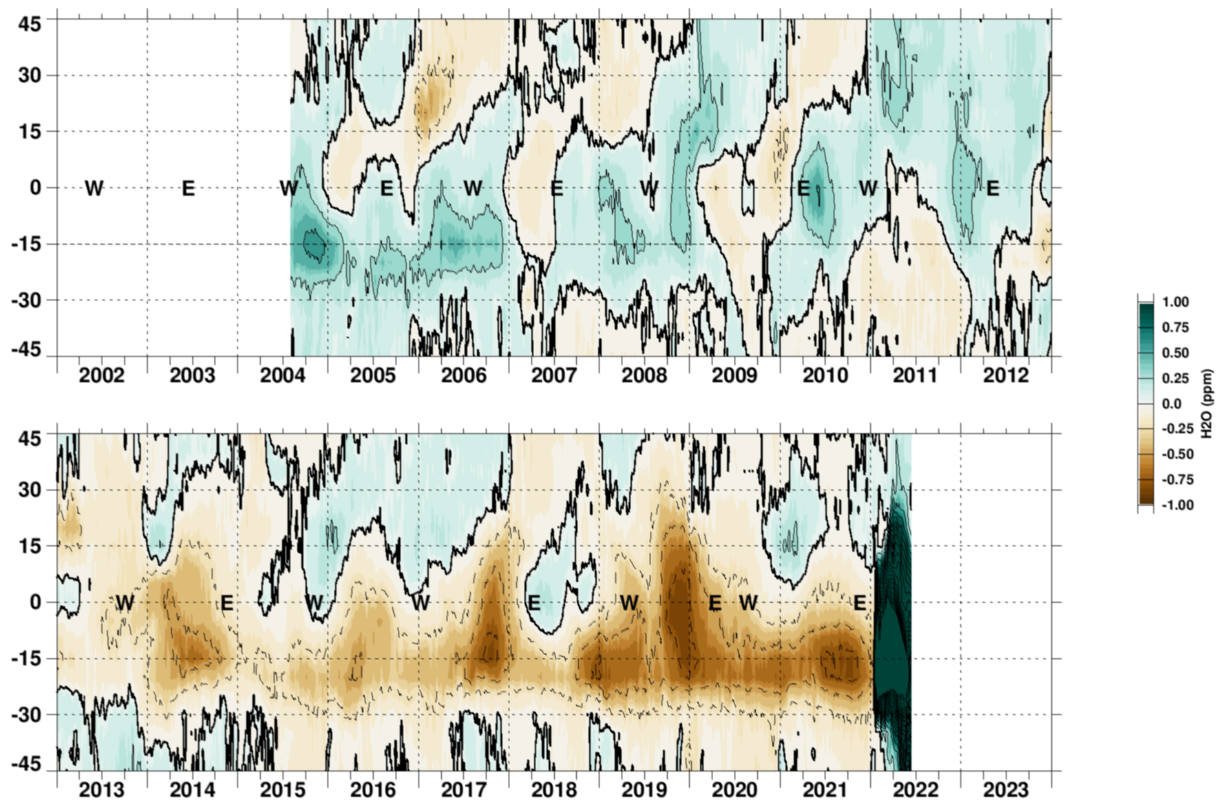

Figure 6. Zonal mean stratospheric water vapor at 26.1 hPa (in ppmv) vs. latitude from Aura/MLS (2004-present) showing the unprecedented SWV anomaly due to the January 2022 HTHH eruption. The plot shows MLS water vapor gridded into 5º latitude bins, with the annual cycle removed, missing data filled with linear interpolation, data detrended, and Gaussian smoothing applied (1/2 amplitude = 10 days) to remove higher frequency structure. The easterly (E) and westerly (W) points are as shown in the Singapore zonal winds and indicate the prevailing phase of the Quasi-biennial Oscillation (QBO) of stratospheric winds, which was easterly in January 2022. The HTHH water vapor has spread into the northern hemisphere (below ~30ºN) but most resides in the southern hemisphere. Source: NASA Goddard QBO website (P.A. Newman & N. Kramarova), https://acd-ext.gsfc.nasa.gov/Data_services/met/qbo/

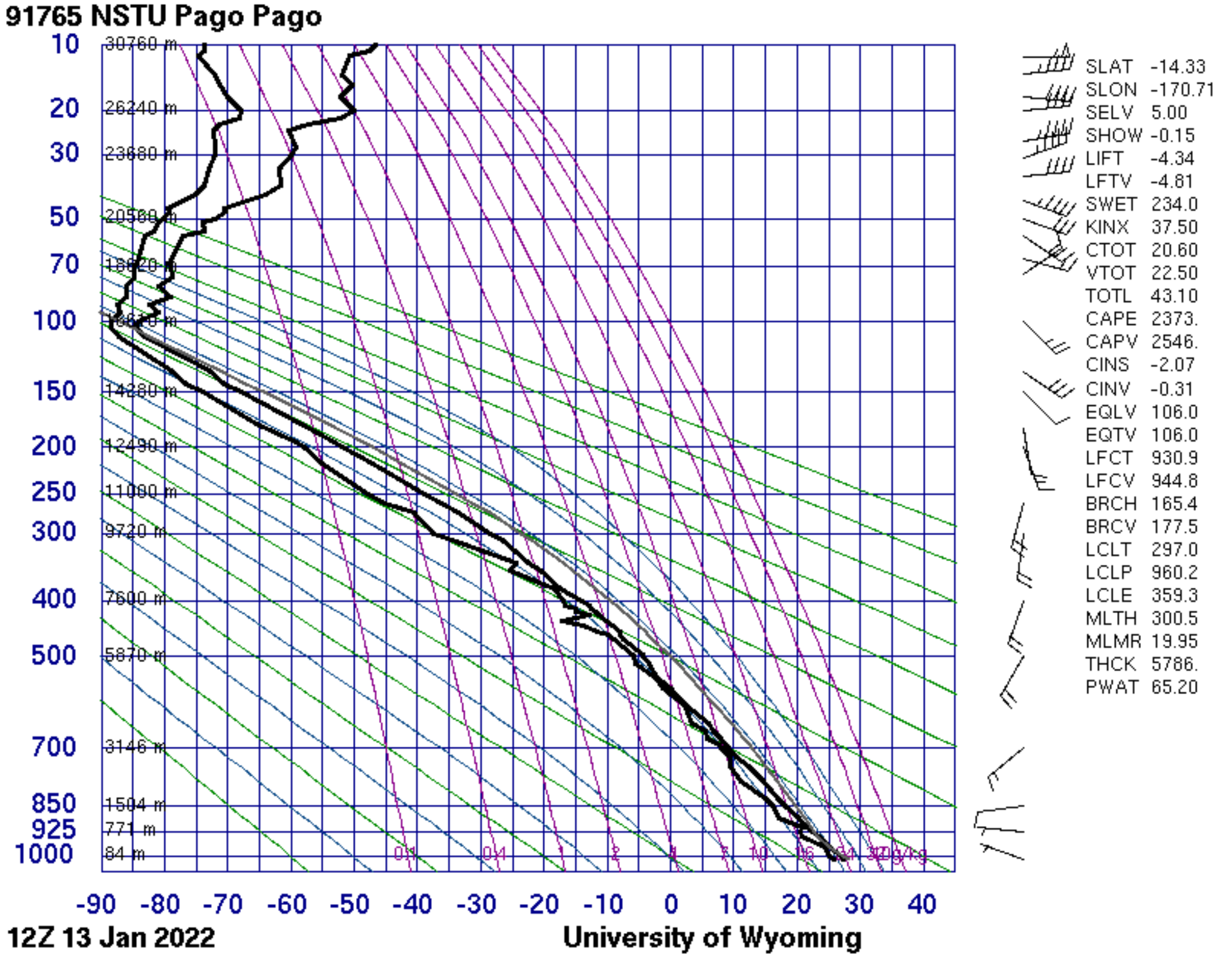

Supplementary Figure S1. Radiosonde sounding from Pago Pago (American Samoa) at 12:00 UTC on January 13, 2022. Source: http://weather.uwyo.edu/upperair/sounding.html.

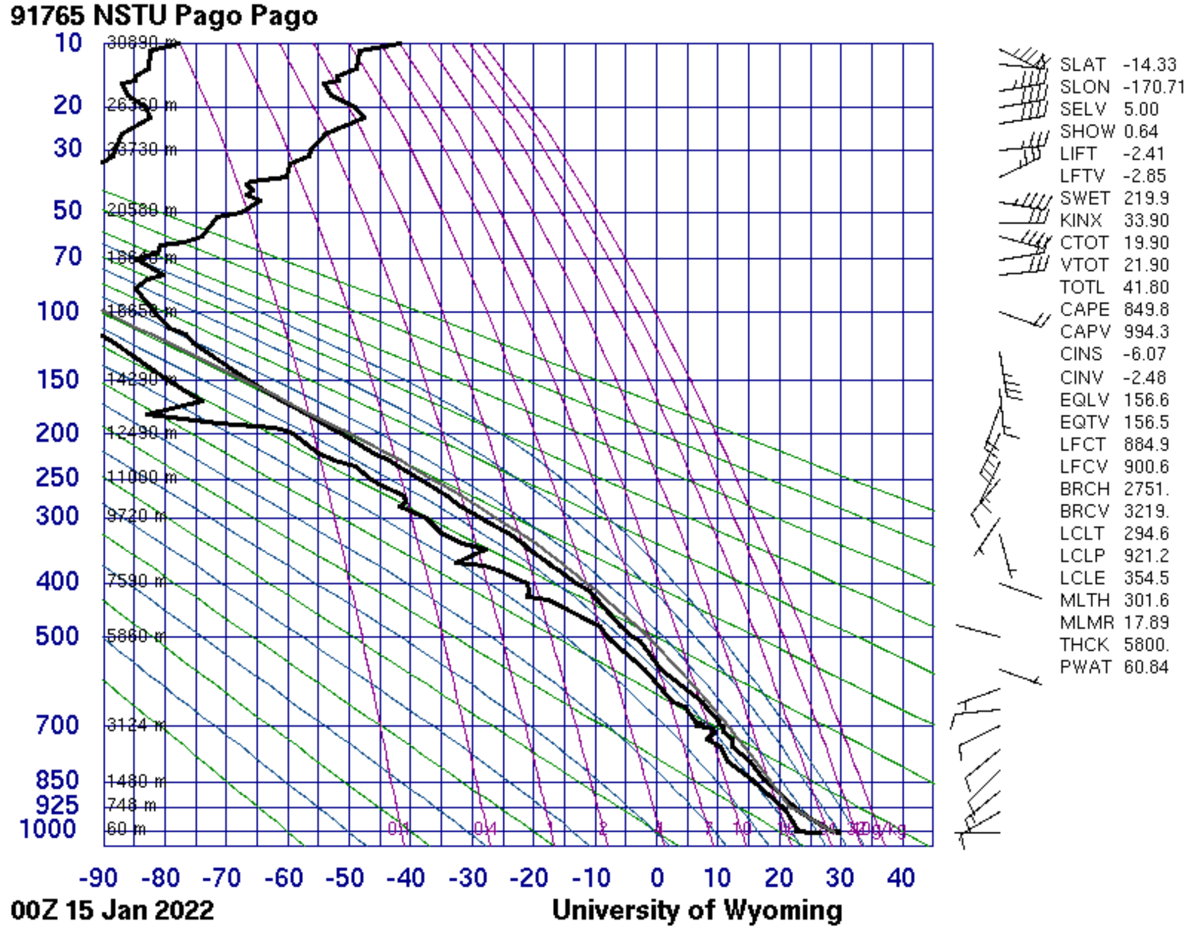

Supplementary Figure S2. Radiosonde sounding from Pago Pago (American Samoa) at 00:00 UTC on January 15, 2022. The sounding plot terminates at ~31 km altitude but the raw data show wind speeds of up to 75 knots (39 m/s) at higher altitudes (~32 km). Source: http://weather.uwyo.edu/upperair/sounding.html.